





Article

Tuning the Properties of Redox-Responsive Chitosan Networks Through Diacid Chain Length and EDC–Carboxylic Acid Molar Ratio

Gabriel Lombardo ^{1,2,3} , Andrés G. Salvay ⁴ , María C. Pagliaricci ³, Norma B. D'Accorso ^{5,6}, Ezequiel Rossi ^{1,2}  and María I. Errea ^{1,2,*} 

- ¹ Instituto Tecnológico de Buenos Aires (ITBA), Lavardén 315, Ciudad Autónoma de Buenos Aires C1437FBG, Argentina; glombardo@itba.edu.ar (G.L.); ezrossi@itba.edu.ar (E.R.)
 - ² Consejo Nacional de Investigaciones Científicas y Técnicas (CONICET), Godoy Cruz 2290, Ciudad Autónoma de Buenos Aires C1425FQB, Argentina
 - ³ YPF Tecnología S.A., Av. del Petróleo s/n, Berisso B1923, Argentina; maria.c.pagliaricci@ypftecnologia.com
 - ⁴ Departamento de Ciencia y Tecnología, Universidad Nacional de Quilmes, Bernal B1876, Argentina; asalvay@unq.edu.ar
 - ⁵ Departamento de Química Orgánica, Facultad de Ciencias Exactas y Naturales, Universidad de Buenos Aires, Ciudad Universitaria, Pabellón 2, Ciudad Autónoma de Buenos Aires C1428EHA, Argentina; norma@qo.fcen.uba.ar
 - ⁶ Consejo Nacional de Investigaciones Científicas y Técnicas (CONICET)-UBA, Centro de Investigación en Hidratos de Carbono (CIHIDECAR), Pabellón 2, Ciudad Autónoma de Buenos Aires C1428EHA, Argentina
- * Correspondence: merrea@itba.edu.ar

Abstract

In this work, redox-responsive chitosan derivatives were prepared by crosslinking with disulfide-bridged dicarboxylic acids. Taking into account that structural variations in diacids can lead to significant differences in properties, especially swelling capacity, this study aimed to evaluate the impact of increasing alkyl chain length and hydrophobicity. Two dicarboxylic acids of different hydrophobic character and chain length were used: dithiodiglycolic acid (DTGA) and dithiopropionic acid (DTPA). The resulting materials were fully characterized. Despite their structural similarity, the derivatives exhibited distinct behaviors: DTGA derivatives formed stable hydrogels, whereas DTPA ones remained compact upon contact with water. These results were confirmed by swelling measurements and oscillatory rheology. The EDC:COOH molar ratio was also evaluated, revealing a strong effect on the degree of crosslinking. Moreover, DTGA systems prepared at a 1:1 ratio showed significantly higher swelling than those synthesized at 3:1. Regarding redox responsiveness, it was assessed by quantifying thiol content before and after reduction with sodium borohydride, and reversibility was assessed through reduction–oxidation cycles. Finally, preliminary experiments evaluated the materials' ability to incorporate benzalkonium chloride as a model biocide, and their release was tested in the presence of thiosulfate-reducing bacteria, providing initial insight into their behavior in redox-responsive delivery systems.

Keywords: redox responsive chitosan; structure–property relationship; disulfide-bridged diacids



Received: 24 July 2025
Revised: 8 August 2025
Accepted: 23 September 2025
Published: 29 September 2025

Citation: Lombardo, G.; Salvay, A.G.; Pagliaricci, M.C.; D'Accorso, N.B.; Rossi, E.; Errea, M.I. Tuning the Properties of Redox-Responsive Chitosan Networks Through Diacid Chain Length and EDC–Carboxylic Acid Molar Ratio. *Polysaccharides* **2025**, *6*, 86. <https://doi.org/10.3390/polysaccharides6040086>

Copyright: © 2025 by the authors. Licensee MDPI, Basel, Switzerland. This article is an open access article distributed under the terms and conditions of the Creative Commons Attribution (CC BY) license (<https://creativecommons.org/licenses/by/4.0/>).

1. Introduction

Chitosan is the partially deacetylated form of chitin, composed of β -(1→4)-*N*-acetyl-D-glucosamine and β -(1→4)-D-glucosamine units (Figure 1) [1]. Its availability from chitin, a highly abundant biopolymer obtained primarily from seafood industry waste, makes it an

attractive candidate for development in line with circular economy principles [2]. Moreover, chitosan is the only naturally occurring polysaccharide with a polycationic character, a property that provides it with distinctive physicochemical behavior and broad application potential [3].

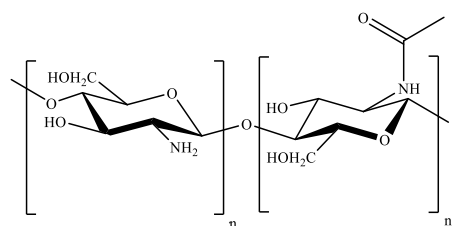


Figure 1. Chemical structure of native chitosan.

Besides, the presence of hydroxyl and amino groups in its structure offers great versatility for chemical modification, enabling the tuning of molecular architecture and bulk properties toward specific purposes [4]. Among various strategies, the covalent crosslinking of chitosan chains via EDC/NHS-mediated amide bond formation with dicarboxylic acids has proven particularly effective in modulating the resulting network structure [5,6]. Regarding the properties of chitosan-based materials, swelling behavior is a critical parameter for many applications, especially in biomedical, pharmaceutical, and environmental fields, as it influences permeability, mechanical stability, and performance [7]. Therefore, differences in swelling capacity between materials can lead to significant variations in their suitability for specific uses. Previous studies have shown that differences in the chemical structure of diacids, such as the presence or absence of hydroxyl groups, can significantly influence the structure and behavior of the resulting materials, even when chain length is held constant [5]. Notably, drastic changes in properties such as swelling have been demonstrated as a result of minimal structural variations in the crosslinkers, specifically the spatial orientation of hydroxyl groups [6]. These findings highlight the relevance of even minimal structural variations in the crosslinkers in determining the final properties of chitosan-based networks.

In this context, the main objective of this work was to investigate the impact of diacid chain length and hydrophobicity on the chemical structure and functional properties of redox-responsive chitosan-based networks. With this aim, chitosan was crosslinked via amide bond formation using dithiodiglycolic acid (DTGA) and dithiopropionic acid (DTPA), two structurally similar dicarboxylic acids that differ only in alkyl chain length, and consequently in hydrophobicity (Figure 2).

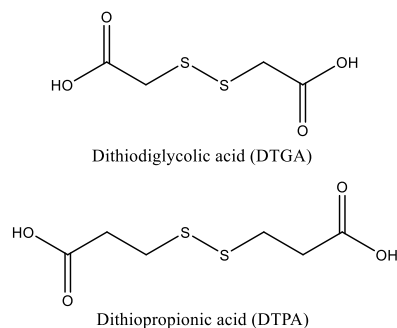


Figure 2. Chemical structure of dithiodiglycolic acid (DTGA) and dithiopropionic acid (DTPA).

Redox-responsive polymers are materials that contain chemical groups capable of undergoing reversible oxidation–reduction reactions in response to the surrounding redox environment [8]. A common design strategy involves the incorporation of disulfide bonds (–S–S–), which remain stable under oxidative conditions but cleave in the presence of

reducing agents, yielding thiol groups ($-SH$) [9]. This reversible cleavage–reformation mechanism provides a useful molecular switch for designing smart delivery systems with controlled release capabilities [10].

These stimulus-sensitive systems have attracted growing interest due to their versatility and ability to respond selectively to reducing environments. This property makes them highly valuable for a wide range of applications. In agriculture, they enable controlled release of pesticides in environments such as flooded rice fields or insect digestive systems, where naturally occurring thiols like glutathione can trigger the cleavage of disulfide bonds and promote active compound release [11,12]. In the oil and gas industry, these materials offer promising strategies to combat thiosulfate-reducing bacteria, a major cause of Microbiologically Influenced Corrosion (MIC) in production systems [13,14]. Moreover, their potential in biomedicine is particularly compelling, especially for targeted drug delivery in cancer therapy, where the intracellular environment of tumor cells presents elevated levels of glutathione compared to healthy tissue, allowing selective activation of therapeutic agents inside malignant cells [15,16].

In addition to investigating the impact of diacid chain length and hydrophobicity on material behavior, this work also aimed to evaluate how variations in the EDC–carboxylic acid molar ratio affect the structure of the resulting polymeric networks. Together, these objectives seek to deepen the understanding of structure–property relationships in redox-responsive chitosan derivatives, contributing to a more rational design of functional materials for targeted applications.

The materials were comprehensively characterized through *FT-IR* and conductometric titration, along with the evaluation of their rheological behavior and swelling capacity. Furthermore, the redox responsiveness of the chitosan derivatives was investigated by monitoring thiol content before and after reduction with sodium borohydride, and their redox reversibility was confirmed through a reduction–oxidation cycle.

Additionally, preliminary experiments were conducted to examine the ability of the chitosan derivatives to incorporate benzalkonium chloride (BAK) as a model biocide. Their responsiveness was subsequently tested in the presence of thiosulfate-reducing bacteria [17], providing initial insight into their behavior in responsive delivery systems.

2. Materials and Methods

2.1. Materials

Native chitosan of medium molecular weight was purchased from Sigma (Sigma-Aldrich 448877, Saint Louis, MO, USA). The degree of deacetylation (DD) of chitosan was assessed by conductometric titration (DD = 70%). 3,3'-dithiodipropionic acid (DTPA), 5,5'-dithiobis(2-nitrobenzoic acid) (DTNB), sodium borohydride, calcium chloride, magnesium chloride, sodium chloride, sodium sulfate and sodium bicarbonate were all reagent grade (Sigma-Aldrich, Saint Louis, MO, USA). Sodium hydroxide and hydrochloric acid were obtained from Merck and were analytical grade. Methanol was HPLC grade (Sintorgan S.A., Villa Martelli B1603, Buenos Aires, Argentina). Monopotassium phosphate and dipotassium phosphate were analytical grade (Anedra, Los Troncos del Talar B1618, Buenos Aires, Argentina). *N*-hydroxysuccinimide (NHS), dithiodiglycolic acid (DTGA) and *N*-ethyl-*N'*-(3-dimethylaminopropyl) carbodiimide hydrochloride (EDC) were all reagent grade (BLD Pharmatech Ltd., Songjiang District, Shanghai, China). Benzalkonium chloride (80%) (Meraquat BZ) was obtained from Meranol (Meranol S.A.C.I., Dock Sud B1871, Buenos Aires, Argentina). Quench-GoneTM Organic Modified Test Kit (QGO-MTM) was acquired from LuminUltra[®] (LuminUltra Technologies Ltd., Fredericton, NB E3G 6M1, Canada).

2.2. Chitosan Functionalization via Disulfide-Containing Diacids

2.2.1. Modification with DTPA

The diacid was incorporated into the chitosan structure via amide bond formation, as was previously described [5,18]. Briefly, a solution of native chitosan (420 mg, 1.69 mmol of amino groups) was prepared in 0.1 M HCl (16.9 mL) under mechanical stirring. In parallel, the sodium salt of DTPA was prepared by dissolving DTPA (178 mg, 1.69 mmol of carboxyl groups) in water (2 mL) together with a stoichiometric amount of sodium bicarbonate (142 mg). The chitosan and DTPA solutions were then combined, and the mixture was cooled to 4 °C in an ice bath. The pH was adjusted to 6.5 with a 0.1 M NaOH aqueous solution. Then, a solution of EDC and NHS in 3 mL of cold water was added. Different EDC:COOH molar ratios (0.5:1, 1:1, 3:1, and 5:1) were tested, maintaining a constant NHS:EDC ratio of 1:1 in all cases. After 7 h of stirring at 4 °C, the mixtures were maintained under static conditions at the same temperature for another 17 h. After that, the reactions were quenched by the addition of 5 mL of a 10% NaOH aqueous solution. The resulting materials were subjected to sequential washing by centrifugation with (i) 0.1 M HCl aqueous solution (until pH 2), (ii) 0.1 M NaOH aqueous solution (until pH 10), and (iii) distilled water (until neutral pH was reached). Finally, all products were freeze-dried. The resulting materials were named ChDTPA0.5, ChDTPA1, ChDTPA3, and ChDTPA5, according to the EDC:COOH ratios (0.5:1, 1:1, 3:1, and 5:1) used in each synthesis.

2.2.2. Modification with DTGA

Based on the results obtained from the DTPA modification, EDC:COOH molar ratios of 1:1 and 3:1 were selected for the reaction of chitosan (420 mg, 1.69 mmol of amino groups) with DTGA (154 mg, 1.69 mmol of carboxyl groups), following the same procedure described above. The products were named ChDTGA1 and ChDTGA3, respectively.

2.3. Chemical Characterization of Chitosan Derivatives

Native chitosan and its derivatives, as obtained after synthesis and purification, were analyzed by Fourier Transform Infrared Spectroscopy (FT-IR) and conductometric titration [19].

The FT-IR spectra were acquired using a Thermo Scientific Nicolet 6700 spectrometer (Thermo Fisher Scientific, Waltham, MA, USA) in transmission mode over the range of 400–4000 cm^{-1} with a resolution of 4 cm^{-1} and 32 scans per sample. Each sample was mixed with KBr as matrix at a mass ratio of 1:100 and pressed into 3 mm discs using a Hand Press accessory (PIKE Technologies, Madison, WI, USA). Spectra were acquired for all derivatives in both their protonated and deprotonated forms. The deprotonated form corresponds to the state of the materials as obtained after synthesis, while the protonated form was prepared by dispersing each material in a 0.1 M HCl aqueous solution followed by freeze-drying.

For the conductometric titration, either native chitosan or its derivatives (150 or 300 mg) were dissolved or dispersed in 0.1 M aqueous HCl (10.0 mL) under magnetic stirring. Subsequently, 25 mL of distilled water was added to the mixture. Titration was performed using a 0.1 M NaOH aqueous solution, while pH and conductivity were recorded at 0.05 mL increments of titrant addition. Measurements were carried out using a Sper Scientific Bench-Top Water Quality Meter 860033 (Sper Scientific, Scottsdale, AZ, USA), equipped with both pH and conductivity probes. The equivalence points were determined as the intersection of the straight-line equations from linear regression on the conductivity vs. volume plots (see Supplementary Materials Figures S1–S7).

The deacetylation degree (% DD) of native chitosan was calculated based on the equivalence points obtained from titration, by applying Equation (1). In this equation, $[NaOH]$ denotes the sodium hydroxide concentration (mol/L), V_1 and V_2 represent the

volumes (L) corresponding to the first and second equivalence points, m is the mass of chitosan used (g), and 203 and 161 are the molar masses (g/mol) of the acetylated and deacetylated monomeric units, respectively.

$$\% DD = \frac{203 \cdot (V_2 - V_1) \cdot [NaOH]}{m + (203 - 161) \cdot (V_2 - V_1) \cdot [NaOH]} \cdot 100\% \quad (1)$$

To determine the molar fraction of each structural unit in the modified chitosan (i.e., acetylated (x_{Ac}), unsubstituted (x_{NH_2}), crosslinked (x_{CL}) and monosubstituted (x_{COOH})), it was assumed that the acetylated moieties remained unaffected under the experimental conditions [20]. The molar proportions of the remaining units were calculated using Equations (2)–(4). In these equations, ΔV_1 and ΔV_2 correspond to the volumes (L) of NaOH consumed between the first and second, and second and third equivalence points, respectively; $[NaOH]$ denotes the sodium hydroxide concentration (mol/L), m is the mass of modified chitosan used (g), and Mr_{COOH} , Mr_{NH_2} , Mr_{CL} and Mr_{Ac} are the molecular weight (g/mol) of each structural unit [5,6].

$$x_{COOH} \cdot \frac{m}{\overline{Mr}} = \Delta V_1 \cdot [NaOH] \quad (2)$$

$$x_{NH_2} \cdot \frac{m}{\overline{Mr}} = \Delta V_2 \cdot [NaOH] \quad (3)$$

$$\overline{Mr} = Mr_{Ac} \cdot x_{Ac} + Mr_{NH_2} \cdot x_{NH_2} + Mr_{COOH} \cdot x_{COOH} + Mr_{CL} \cdot x_{CL} \quad (4)$$

2.4. Swelling Experiments

The water absorption capacity of all derivatives, as obtained after synthesis and purification, was determined by placing 25.0 mg of each material in a cone-shaped folded filter paper. The cones containing the samples were then immersed in water-containing tubes. After 10 min, they were removed and left to drain the excess water for another 10 min. Finally, each cone was weighed, and swelling was calculated according to Equation (5) [21]. This immersion, draining, and weighing process was repeated 20 times for each sample.

$$\% \text{ swelling} = \frac{\text{swelled weight} - \text{dry weight}}{\text{dry weight}} \cdot 100 \quad (5)$$

2.5. Rheological Studies

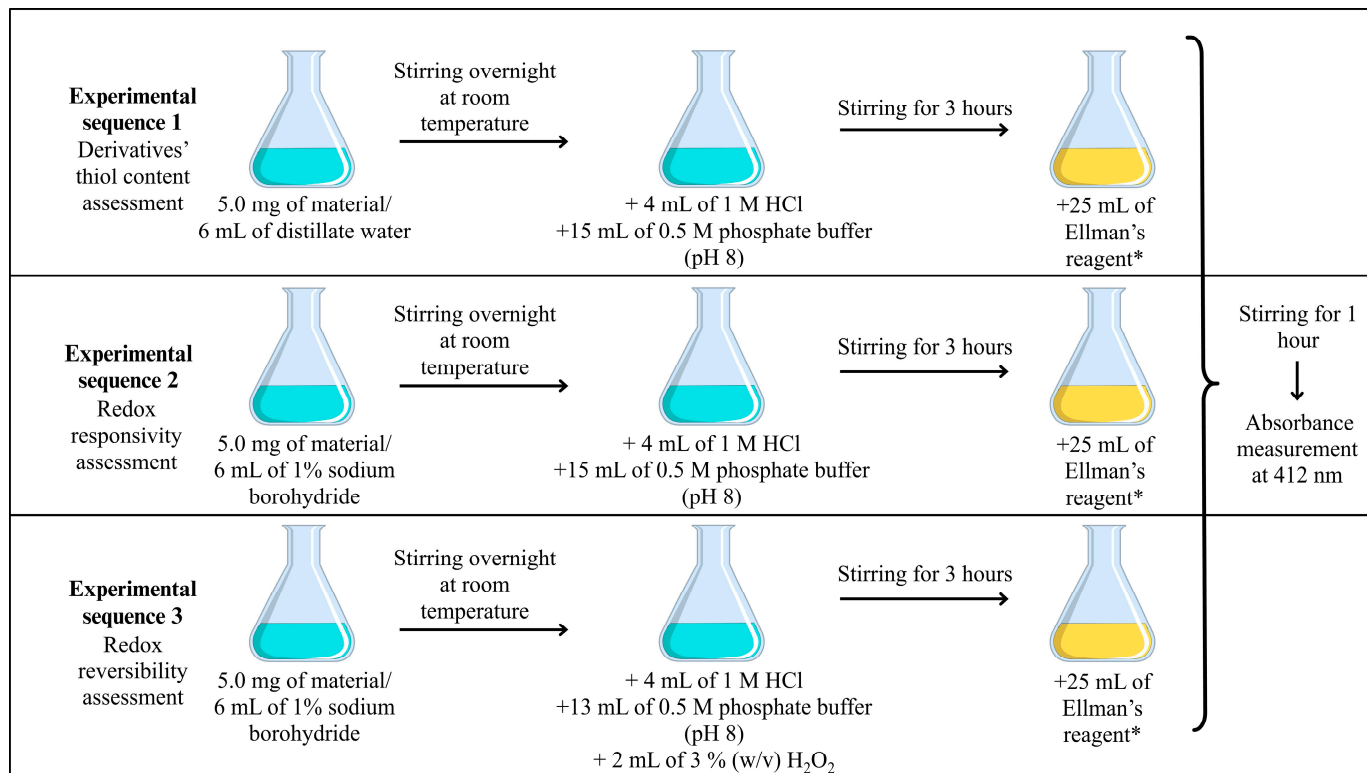
The viscoelastic behavior of the hydrogels, prepared from the freeze-dried polymers obtained after synthesis and purification, was assessed using oscillatory rheological tests carried out on an AR-G2 rheometer (TA Instruments, New Castle, DE, USA). A parallel plate configuration made of steel (40 mm diameter, 800 μ m gap) was employed. For each run, 1 mL of the hydrated sample was positioned between the plates, and the tests were conducted at 34 $^{\circ}$ C.

Strain sweep tests were performed within a deformation range of 0.01% to 100% at a constant angular frequency of 1 rad/s to determine the linear viscoelastic region (LVR). Frequency sweep experiments were then carried out from 0.1 to 100 rad/s at a fixed strain amplitude of 0.5%. The storage modulus (G') and loss modulus (G'') were recorded as a function of strain or angular frequency, depending on the test. All measurements were performed in triplicate, and one representative curve per sample was selected for analysis.

2.6. Assessment of the Polymer's Redox Responsiveness

Redox responsiveness was evaluated by comparing the thiol content of the samples before and after reduction with sodium borohydride [22]. In a separate experiment, redox reversibility was assessed by comparing the thiol content of the original sample with

that of a sample subjected to a reduction–oxidation sequence involving sodium borohydride reduction followed by hydrogen peroxide oxidation [23]. In all cases, thiol content was determined using the Ellman assay, and the experimental conditions are detailed in Scheme 1 [22]. All assays were performed in triplicate, and the results are presented as mean \pm standard deviation.



Scheme 1. General procedure for redox-responsiveness testing of chitosan derivatives. * 0.03% DTNB in 0.5 M phosphate buffer (pH 8).

2.7. Preliminary Application Insights: Biocide Entrapment Studies

Under pre-loading conditions [23,24], benzalkonium chloride (0.845 mmol) was added to the chitosan–diacid reaction mixture (Section 2.2) one hour after EDC addition, at a BAK: carboxylic acid molar ratio of 1:1.

Entrapment efficiency (Equation (6)) was calculated as the difference between the amount of biocide initially added to the reaction (q_0) and the total amount of free biocide recovered (q_r), which was obtained by summing the quantities of biocides detected in the reaction medium and in all washing solutions [24].

$$\text{Entrapment efficiency (\%)} = \frac{q_0 - q_r}{q_0} \cdot 100 \quad (6)$$

The concentration of BAK was determined by HPLC using a Zorbax Eclipse XDB-C18 (Santa Clara, CA 95051, USA) column (4.6 \times 250 mm, 5 μ m) using an external calibration curve (10–400 mg/L). Chromatographic analyses were carried out at 50 $^{\circ}$ C employing a mobile phase composed of methanol and phosphate buffer (100 mM, pH 3) in a 70:30 ratio (v/v) [25].

All experiments were conducted in duplicates, and the results are presented as mean \pm standard deviation.

2.8. Kill Test Assays Against Thiosulfate-Reducing Bacteria

An enriched *Halanaerobium* culture was provided by YPF Tecnología (YPF Tecnología S.A., Berisso B1923, Buenos Aires, Argentina), obtained by filtering flowback water of unconventional Oilfield in Argentina and cultivating the microorganisms in a modified version of Jones's medium [26,27].

To prepare the test samples, 4 mL of *Halanaerobium* starting culture (1×10^8 ME/mL) were diluted in a Falcon tube with 36 mL of test medium, prepared by mixing equal volumes of sterilized saline solutions A and B (Table 1). Then, a mass of chitosan derivative containing biocide was added to match a final BAK concentration of 15 mg/L, based on the entrapment efficiency of each material. In all cases, this corresponded to approximately 4 mg of polymer. A parallel test was conducted using commercial BAK at the same final concentration (15 mg/L). For each material, a control sample containing the same amount of chitosan derivative without biocide was also included. Additionally, a blank assay consisting only of the bacterial suspension in saline solution was used as a reference.

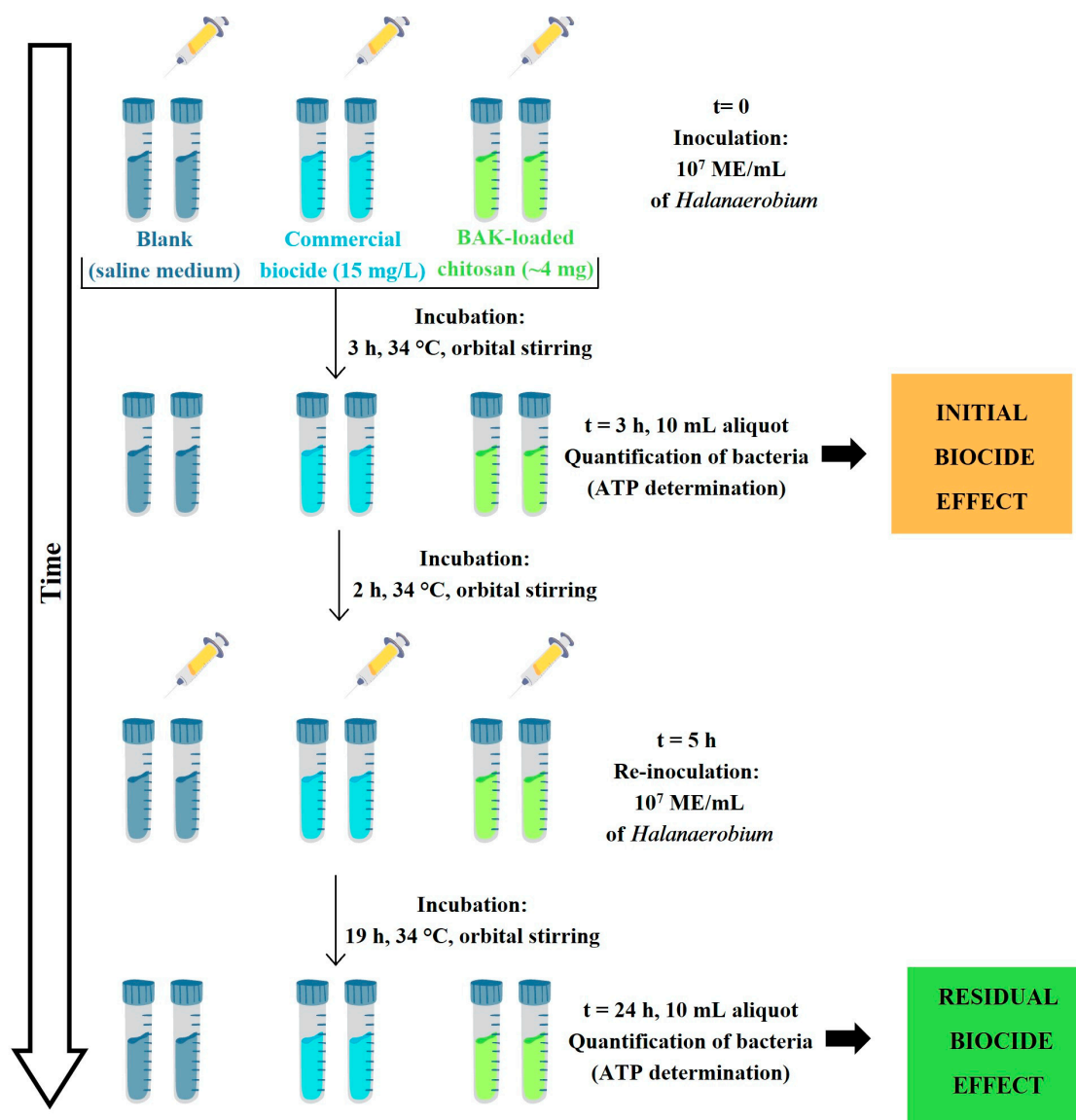
All samples were incubated at 34 °C with orbital shaking for 3 h, after which microbial concentration was quantified on a 10 mL aliquot. After 5 h of total incubation, 4 mL of fresh starter culture and 6 mL of sterile test medium were added to each tube, and incubation was continued for an additional 19 h. Microbial concentration was again determined at the end of the incubation period.

In all cases, the total viable count (TVC) of microorganisms was indirectly determined by measuring the ATP content using a Quench-Gone™ Organic Modified test kit (QGO-M, LuminUltra®) (LuminUltra Technologies Ltd., Fredericton, NB E3G 6M1, Canada), following the ASTM D7687 standard method [28]. Results were expressed as microbial equivalents per milliliter (ME/mL), based on ATP bioluminescence calibrated to *E. coli* equivalents, as specified by the manufacturer.

All experiments were carried out in duplicates, and the results are presented as mean \pm standard deviation. A scheme of the procedure is shown in Scheme 2.

Table 1. Composition of solutions A and B for the biocide experiments against *Halanaerobium*.

Solution A	Concentration (%w/v)
CaCl ₂	3.32
MgCl ₂	4.75
Solution B	Concentration (%w/v)
Na ₂ SO ₄	0.30
NaHCO ₃	0.24
NaCl	26.36



Scheme 2. Experimental procedure for the kill tests against thiosulfate-reducing bacteria.

3. Results and Discussion

3.1. Effect of EDC:COOH Ratio on the Reaction Between Chitosan and DTPA

The covalent coupling between chitosan and dithiodipropionic acid (DTPA) was achieved via amide bond formation using the EDC:NHS activation system, as mentioned in the Introduction Section. To evaluate the influence of coupling conditions on the reaction outcome, different EDC:COOH molar ratios (0.5:1, 1:1, 3:1, and 5:1) were tested. In the presence of dicarboxylic acids, two types of substitution can occur: (i) crosslinking, when both carboxyl groups react with amino groups from different chitosan chains, and (ii) monosubstitution, when only one carboxyl group participates in the reaction, leaving the other free (Figure 3). The relative extent of these two pathways depends not only on the efficiency of carboxyl activation and the availability of reactive amino groups on the chitosan backbone but also on the length and/or flexibility of the diacid chain, which can modulate the extent of interchain crosslinking.

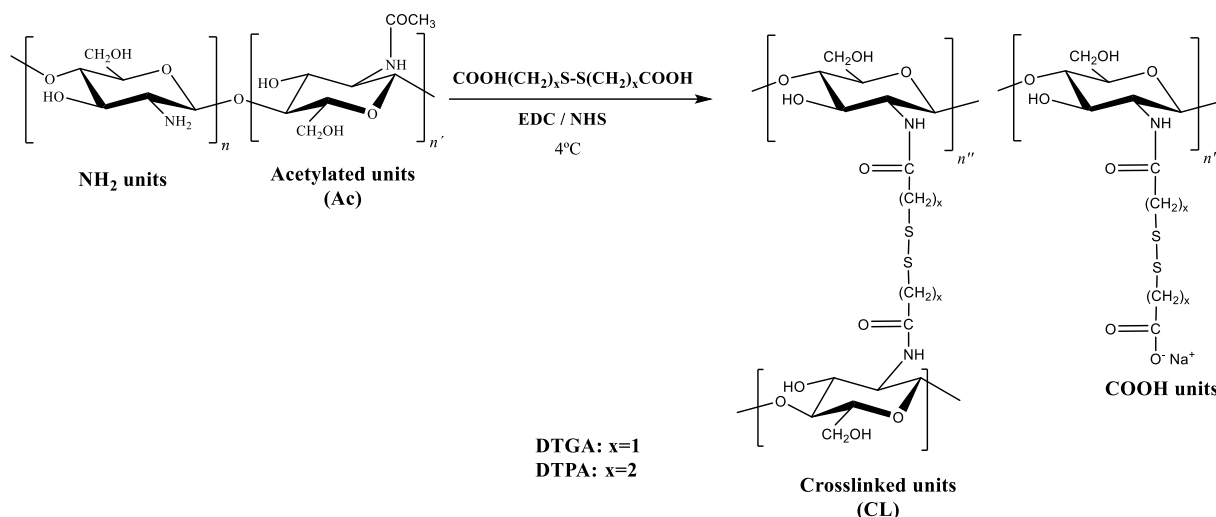


Figure 3. Scheme of the covalent crosslinking between chitosan and disulfide-bridged dicarboxylic acids (DTGA or DTPA) via EDC/NHS-mediated amide bonds.

Strong evidence for the covalent grafting of DTPA into the chitosan backbone via amide bond formation was obtained through *FT-IR* spectroscopy for all the EDC:COOH molar ratios tested. Compared to native chitosan, all modified samples showed a marked increase in the intensity of the signals at 1650 , 1558 , and 1204 cm^{-1} , corresponding to C=O stretching, N–H bending, and C–N stretching vibrations, respectively, of newly formed secondary amide groups [29]. Additionally, the near-complete disappearance of the N–H scissoring band at 1602 cm^{-1} (evident in the spectrum of native chitosan (Figure 4a)) further supports the successful incorporation of DTPA via amide bond formation.

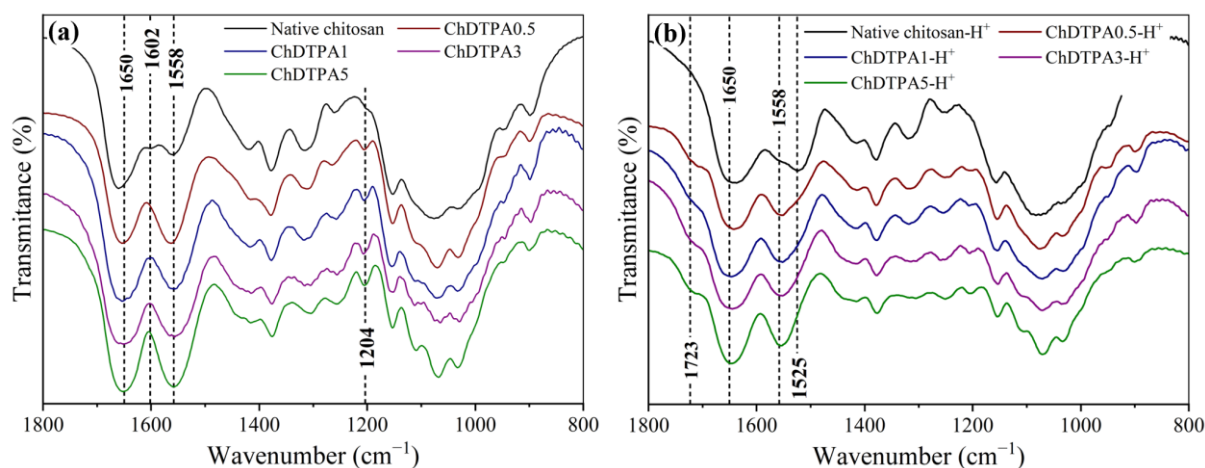


Figure 4. *FT-IR* spectra of native chitosan, ChDTPA0.5, ChDTPA1, ChDTPA3 and ChDTPA5 in their (a) deprotonated and (b) protonated forms.

However, to assess whether monosubstitution had occurred (i.e., incorporation of DTPA units through only one carboxyl group, leaving the other unreacted), it was necessary to detect the C=O stretching of free carboxylic acid groups. This signal serves as a key spectroscopic marker, since it allows distinguishing between fully crosslinked units and those where only one carboxyl group reacted, leaving the other free. In the deprotonated form, the C=O stretching of carboxylate groups overlaps with the amide bands, making it indistinguishable. Therefore, spectra were also recorded in the protonated form after acid treatment. Upon protonation, the C=O stretching of the carboxylic acid shifts to higher wavenumbers, allowing its differentiation [6]. Under these conditions, the appearance of a

distinct peak at 1729 cm^{-1} , along with a decrease in the intensity of the 1558 cm^{-1} band, confirmed the presence of unreacted COOH groups in all samples studied (Figure 4b), indicating that at least some monosubstitution had taken place.

To further elucidate the substitution pattern of the materials, conductometric acid–base titration was performed, allowing the quantification of unsubstituted amino groups, mono-substituted units, and crosslinked structures (titration curves are shown in Supplementary Materials, Figures S2–S5). Results are summarized in Table 2. In all products, a high degree of substitution was observed, as evidenced by a substantial decrease in the amount of free amino groups with respect to native chitosan. Regarding the EDC:COOH molar ratio, the 0.5:1 and 1:1 ratios led to similar and comparatively lower degrees of substitution, whereas the 3:1 and 5:1 ratios resulted in higher and also comparable substitution levels. Concerning the crosslinking degree, increasing the proportion of EDC led to a significant enhancement of this structural parameter. Notably, at the lowest ratio tested (0.5:1), only monosubstitution was detected, with no evidence of crosslinked units. This finding is particularly relevant when considering potential redox-responsive applications. Since the mechanism of responsiveness involves the cleavage of disulfide bridges under reducing conditions, allowing, for instance, the release of entrapped active compounds, a crosslinked architecture is essential. Materials containing only monosubstituted units lack this feature and are therefore not suitable for such purposes.

On the other hand, no significant differences were observed between the 3:1 and 5:1 ratios, suggesting that crosslinking levels reached a plateau beyond a certain EDC excess. Based on these observations, the 1:1 and 3:1 EDC:COOH ratios were selected for all subsequent studies, as they provided representative examples of low and high crosslinking degrees, respectively. The 5:1 ratio was not further considered, as it implied an unnecessary consumption of reagent without clear structural or functional benefits.

Table 2. Structural units determined by conductometric titration for native chitosan and its DTPA-derivatives.

Sample	Acetylated Units (%)	-NH ₂ Units (%)	Crosslinked Units (%)	-COOH Units (%)
Native chitosan	30 ± 2	70 ± 2	--	--
ChDTPA0.5	30 ± 2	26 ± 2	0 ± 3	44 ± 2
ChDTPA1	30 ± 2	27 ± 2	20 ± 3	23 ± 2
ChDTPA3	30 ± 2	17 ± 2	34 ± 3	19 ± 2
ChDTPA5	30 ± 2	15 ± 2	35 ± 3	20 ± 2

3.2. Chitosan Crosslinking with DTGA

To assess how the total chain length of the disulfide crosslinker affects the substitution pattern and crosslinking efficiency, new derivatives were synthesized using dithiodiglycolic acid (DTGA, 6 atoms total, including the disulfide bridge) and compared with the previously studied dithiodipropionic acid (DTPA, 8 atoms). Reactions were carried out using EDC:COOH molar ratios of 1:1 and 3:1, selected as representative conditions for moderate and high crosslinking, respectively.

Regarding the chemical characterization, the FT-IR spectra of the DTGA-based materials closely resembled those of the DTPA-modified samples, showing clear evidence of amide bond formation (Figure 5). The characteristic bands of secondary amide groups appeared with increased intensities at 1657 , 1558 , and 1204 cm^{-1} , relative to native chitosan, indicating efficient covalent functionalization. These spectral features, together with the marked reduction in the band associated with free amino groups, suggest a high degree of substitution in the resulting materials. Spectra were recorded in both protonated and de-

protonated forms, as done previously with the DTPA derivatives, to allow a comprehensive analysis of the chemical structure, as previously discussed.

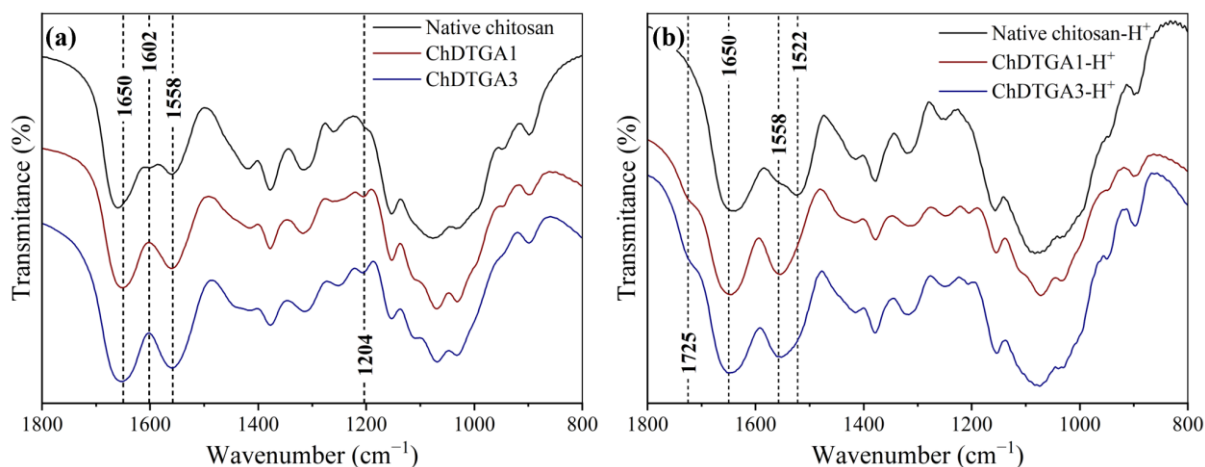


Figure 5. FT-IR spectra of native chitosan, ChDTGA1 and ChDTGA3 in their (a) deprotonated and (b) protonated forms.

The analysis of the structural units in the DTGA-based materials was carried out by conductometric acid–base titration, following the same procedure previously applied to the DTPA series, as discussed in the preceding section. Titration curves are shown in Supplementary Materials, Figures S6 and S7, and results are shown in Table 3.

Compared to DTPA, the shorter and less flexible DTGA led to reduced crosslinking at a 1:1 EDC:COOH ratio (12% vs. 20%), but this difference was no longer observed at 3:1, where both crosslinkers yielded similar crosslinking degrees (30% vs. 34%). This behavior may be attributed to the lower accessibility of the second carboxyl group in DTGA, which may reduce its chances of reacting before hydrolysis occurs. When EDC is present in excess, reactivation of hydrolyzed groups becomes more likely, allowing crosslinking to proceed more efficiently. Thus, the shorter chain and reduced flexibility of DTGA may limit crosslink formation under equimolar conditions, a limitation that can be overcome by increasing the amount of coupling agent.

Table 3. Structural units determined by conductometric titration for chitosan derivatives crosslinked with DTGA and DTPA under selected conditions.

Sample	Acetylated Units (%)	-NH ₂ Units (%)	Crosslinked Units (%)	-COOH Units (%)
ChDTGA1	30 ± 2	26 ± 2	12 ± 3	32 ± 2
ChDTGA3	30 ± 2	19 ± 2	30 ± 3	21 ± 2
ChDTPA1	30 ± 2	27 ± 2	20 ± 3	23 ± 2
ChDTPA3	30 ± 2	17 ± 2	34 ± 3	19 ± 2

3.3. Assessment of the Polymer's Redox Responsiveness

Redox responsiveness of the materials was evaluated by measuring the thiol content in two conditions: (i) the original (untreated) materials and (ii) after reduction with NaBH₄. Additionally, to assess redox reversibility, a separate test was conducted in which the samples were subjected to sequential reduction with NaBH₄ and reoxidation with hydrogen peroxide [23]. The results are summarized in Table 4.

Table 4. Results of the redox responsiveness assays. Values are expressed as mean \pm standard deviation ($n = 3$). “Not detectable” indicates that the thiol content was below the detection limit of the method.

Sample	Thiol Content ($\mu\text{mol/g}$ of Polymer)		
	Non-Reduced	Reduced	Re-Oxidized
ChDTPA1	Not detectable	1000 ± 300	Not detectable
ChDTGA1	Not detectable	1100 ± 100	Not detectable
ChDTPA3	Not detectable	900 ± 200	Not detectable
ChDTGA3	Not detectable	1400 ± 100	Not detectable

In all cases, the materials exhibited clear redox responsiveness, as shown by the significant increase in thiol content upon reduction and its subsequent decrease after reoxidation. These results demonstrate that the disulfide crosslinks introduced into the chitosan network are efficiently cleaved under reducing conditions and can be re-formed upon oxidation. However, since comprehensive structural analyses were not performed after redox cycling, we cannot conclusively confirm full reversibility of the network architecture.

3.4. Evaluation of Swelling Behavior and Rheological Performance of Chitosan Derivatives

The DTGA-crosslinked derivatives exhibited a hydrogel-like appearance in the swollen state, whereas the DTPA-crosslinked materials showed a more compact morphology in both dry and swollen states (Figure 6).

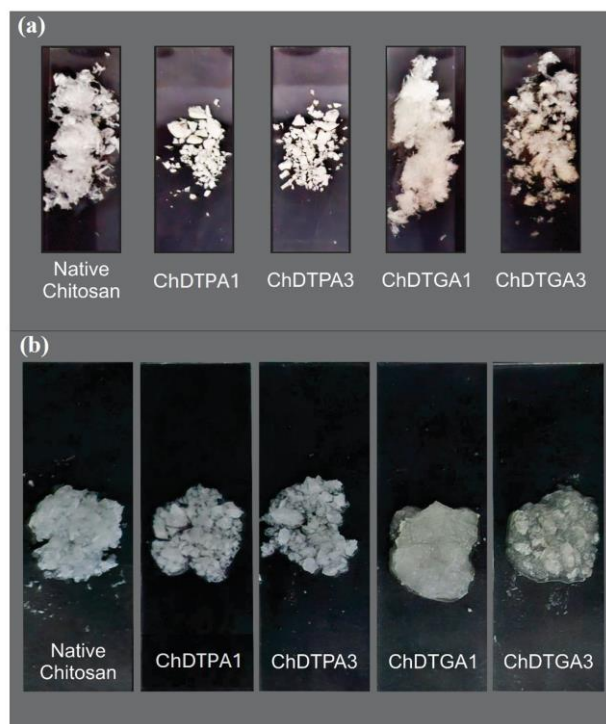


Figure 6. Native chitosan and the disulfide-crosslinked derivatives in their (a) dry and (b) swollen states.

All materials (ChDTGA1, ChDTGA3, ChDTPA1, and ChDTPA3) were insoluble in water across the entire pH range. Swelling behavior was evaluated both qualitatively and quantitatively. Figure 7a shows photographs of 50 mg (dry mass) of each crosslinked chitosan derivative after reaching their maximum swelling capacity upon immersion in water, compared to native chitosan. Quantitative swelling values are presented in Figure 7b.

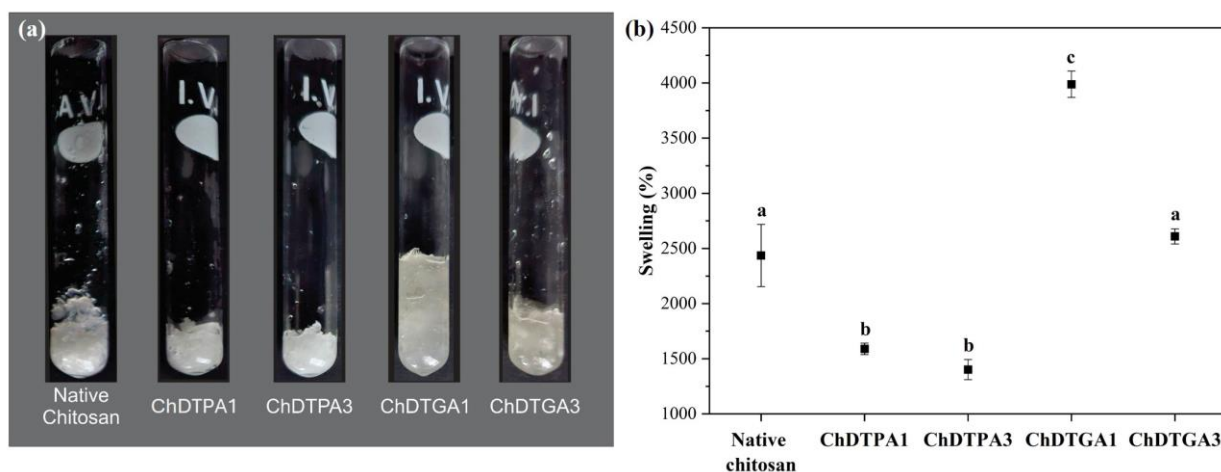


Figure 7. (a) Chitosan derivatives (50 mg of dry polymers) in their swollen state. (b) Swelling capacity of native chitosan and its derivatives. Statistically significant differences ($p \leq 0.05$) between values are indicated by different letters, based on Tukey's HSD post hoc test.

As observed, both qualitatively in Figure 7a and quantitatively in Figure 7b, all DTPA-crosslinked derivatives exhibited significantly lower swelling compared to native chitosan. This reduced swelling is consistent with their more compact solid-state morphology and the absence of hydrogel-like characteristics upon hydration (Figure 6b). In contrast, the DTGA-crosslinked derivatives displayed a hydrogel-like appearance when swollen (Figure 6), along with higher swelling values than their DTPA counterparts. Comparing the DTGA derivatives to native chitosan, ChDTGA3 showed swelling similar to chitosan, whereas ChDTGA1 exhibited significantly greater swelling, which can be attributed to its lower degree of crosslinking.

Overall, the higher hydrophobicity of DTPA reduces its compatibility with water [30], leading to lower swelling, while the degree of crosslinking, as is well known, limits water uptake, resulting in decreased swelling [18].

The viscoelastic properties of the DTGA-crosslinked chitosan derivatives were evaluated using oscillatory rheology tests, and the results are presented in Figure 8. The initial rheological analysis examined how the elastic (G') and viscous (G'') moduli varied with shear strain under a fixed angular frequency of 1 rad/s (Figure 8a). Both samples displayed a linear viscoelastic region between 0.02% and 1% strain, within which both G' and G'' remained nearly constant. Moreover, G' was consistently higher than G'' in this region for both samples, indicating a predominantly elastic behavior [6,18]. These results confirm that both DTGA-crosslinked derivatives behave as viscoelastic solids with a gel-like structure [31,32].

In addition, the frequency dependence of the elastic (G') and viscous (G'') moduli was evaluated at a fixed strain amplitude of 0.5% (Figure 8b). This amplitude was selected to simulate slow deformation processes over extended timescales or under near-static conditions. Throughout the entire angular frequency range, G' remained consistently higher than G'' for both samples, indicating predominant elastic, solid-like behavior [33,34]. In addition, the G' values were higher for sample ChDTGA3, suggesting greater stiffness [35], which is consistent with its higher crosslinking density. Sample ChDTGA1 displayed nearly constant and parallel values of G' and G'' throughout the frequency range, characteristic of typical gel-like material [6,18]. In contrast, ChDTGA3 showed an increase in G' with rising frequency, reflecting a more pronounced solid-like response. A similar trend has been reported for chemically crosslinked hydrogels based on poly(vinyl alcohol)–Fe(III) complexes, where the frequency-dependent increase in G' was attributed to higher crosslinking

density [36]. The reduced swelling capacity of the ChDTGA3 sample, in addition to its higher crosslinking density, may also contribute to this behavior.

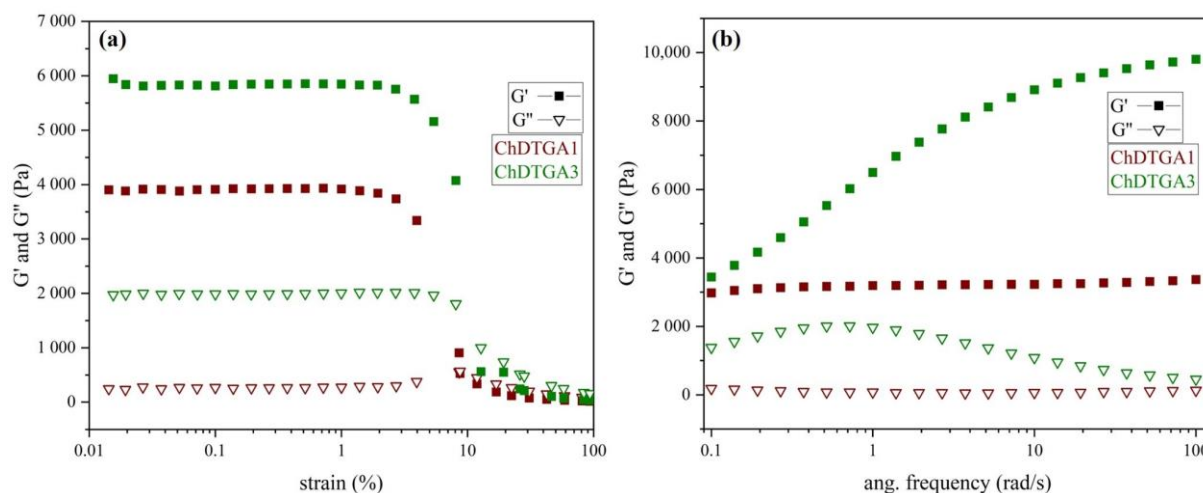


Figure 8. Rheological properties of ChDTGA1 and ChDTGA3 at constant (a) strain and (b) frequency.

3.5. Evaluation of BAK Entrapment as a Functional Test of the Chitosan Derivatives

The biocide entrapment, as described in Section 2.7, was performed under pre-loading conditions, i.e., during the synthesis step. Entrapment efficiency was calculated according to Equation (6) as the difference between the amount of biocide initially added to the reaction medium and the total amount of free biocide recovered from the reaction medium and all washing solutions after synthesis, expressed as percentage. Based on this percentage, the amount of biocide retained per gram of polymer was also calculated. Table 5 presents the corresponding results.

Table 5. Entrapment efficiency and BAK loading (relative to dry polymer mass) in crosslinked chitosan derivatives.

Chitosan Derivative	Entrapment Efficiency (%)	BAK Loading (mg/g of Polymer)
ChDTPA1	43	260 ± 20
ChDTGA1	24	140 ± 20
ChDTPA3	62	270 ± 20
ChDTGA3	41	190 ± 20

The results showed that biocide loading was significantly higher in the DTPA-crosslinked derivatives compared to those crosslinked with DTGA. This could be explained by the higher hydrophobic character of DTPA, associated with its longer aliphatic chain, which may enhance interactions with the hydrophobic domains of BAK [30].

3.6. Kill Test

A kill test is a microbiological assay used to assess the antimicrobial efficacy of a material or compound by evaluating its ability to eliminate or inhibit the growth of microorganisms under controlled conditions [37]. These experiments typically involve exposing a bacterial culture to the biocide in a fluid medium that simulates the target application environment. For example, in the oil & gas industry, biocide performance tests are often conducted in saline solutions to mimic the chemical composition of flowback fluids from hydraulic fracturing operations [27].

In this study, BAK-loaded chitosan derivatives were tested against *Halanaerobium*, a thiosulfate-reducing bacterium considered a major contributor to Microbiologically Induced Corrosion (MIC) in industrial settings. The performance of these materials was compared to that of a commercial biocide at an equivalent BAK dose.

To evaluate the immediate antimicrobial effect, bacterial concentration was quantified 3 h after inoculation. The results showed that the biocidal activity of the BAK-loaded chitosans was comparable to that of the commercial product, indicating that incorporation into the polymer matrix did not impair the short-term efficacy of BAK (Figure 9).

To assess the long-term antimicrobial effect, a fresh inoculum was added 5 h after the initial inoculation, and bacterial concentration was measured again after 24 h. The results confirmed that the prolonged activity of BAK was preserved in the polymer-based formulations, demonstrating sustained biocidal performance over time.

These findings are particularly relevant when considering the use of more labile or environmentally sensitive active agents. The fact that BAK retained its performance when incorporated into the chitosan matrix suggests that this strategy could offer a protective effect, shielding the biocide from potential degradation. This could be especially advantageous in scenarios where degradation of the free compound would otherwise require overdosing to maintain efficacy. Therefore, encapsulation or pre-loading within a polymer matrix may serve not only to sustain antimicrobial performance but also to enhance stability and reduce the required dosage of sensitive active ingredients.

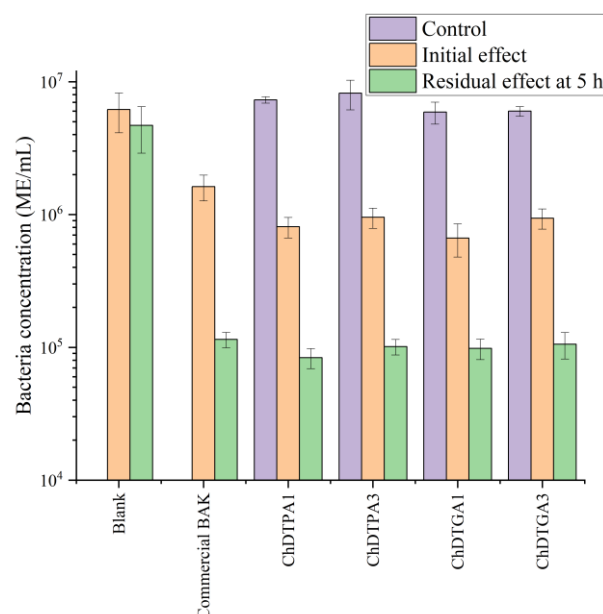


Figure 9. Biocidal activity of benzalkonium chloride-loaded chitosan derivatives against *Halanaerobium*. Control samples correspond to non-loaded chitosan derivatives. The blank consists of the bacterial suspension in saline solution without any material added.

4. Conclusions

In this work, redox-responsive polymers were successfully synthesized by covalently crosslinking chitosan with disulfide-bridged dicarboxylic acids of varying chain lengths. The contrasting behaviors observed between DTGA- and DTPA-crosslinked derivatives highlight the critical influence of alkyl chain length and hydrophobicity on key physico-chemical properties, including swelling capacity and hydrogel formation. Additionally, the EDC:COOH molar ratio significantly affected the degree of crosslinking, thereby modulating swelling behavior. These findings emphasize the importance of deliberate crosslinker

selection and precise stoichiometric control to tailor the responsiveness and functional performance of chitosan-based materials.

Redox responsiveness was supported through reduction–oxidation cycles, which suggest the cleavage and reformation of disulfide bonds, although full reversibility of the network architecture remains to be demonstrated. Preliminary tests also showed the materials' ability to load and release a model biocide under reductive conditions. These results indicate potential applications in agriculture, water treatment, and biomedicine, where selective redox-responsive delivery can enhance efficacy and reduce side effects.

This work demonstrates how variations in crosslinker structure directly influence network architecture and functional properties, highlighting the importance of a structure–property approach in designing chitosan derivatives. It shows that rational crosslinker design is a powerful strategy to fine-tune redox responsiveness and overall functional performance of chitosan-based hydrogels. This approach provides a valuable framework for developing smart materials tailored to specific stimuli and application requirements.

While this study focused on model compounds and in vitro evaluations, future work should assess these materials in more complex environments and with a broader range of active agents. Such investigations will facilitate targeted optimization of material properties for diverse practical applications.

Supplementary Materials: The following supporting information can be downloaded at: <https://www.mdpi.com/article/10.3390/polysaccharides6040086/s1>. Figure S1: Conductometric titration curve of native chitosan; Figure S2: ChDTPA0.5 conductometric titration curve; Figure S3: ChDTPA1 conductometric titration curve; Figure S4: ChDTPA3 conductometric titration curve; Figure S5: ChDTPA5 conductometric titration curve; Figure S6: ChDTGA1 conductometric titration curve; and Figure S7: ChDTGA3 conductometric titration curve.

Author Contributions: Conceptualization, M.I.E.; formal analysis, G.L., A.G.S., E.R.; funding acquisition, M.I.E.; investigation, G.L., A.G.S.; methodology, G.L., A.G.S., M.C.P., E.R., M.I.E.; project administration, E.R., M.I.E.; resources, M.I.E.; supervision, N.B.D., E.R., M.I.E.; visualization, G.L., E.R.; writing—original draft, G.L., A.G.S., M.C.P., E.R., M.I.E.; writing—review and editing, G.L., N.B.D., E.R., M.I.E. All authors have read and agreed to the published version of the manuscript.

Funding: This research was funded by Agencia Nacional de Promoción Científica y Tecnológica (PICT2020-00221), Consejo Nacional de Investigaciones Científicas y Técnicas (CONICET) (PIP 2023-2025 GI-11220220100533CO) and Instituto Tecnológico de Buenos Aires (ITBA).

Data Availability Statement: The original contributions presented in this study are included in the article/Supplementary Material. Further inquiries can be directed to the corresponding author(s).

Acknowledgments: Gabriel Lombardo has a fellowship from YPF-Tecnología (Y-TEC) and CONICET. The authors acknowledge the financial assistance of ITBA and YPF-Tecnología.

Conflicts of Interest: María Clara Pagliaricci was employed by YPF Tecnología S.A. Gabriel Lombardo is not employed by the company. His PhD fellowship is funded by CONICET with additional support from Y-TEC, as part of the company's commitment to the training of new researchers. Therefore, there is no employment relationship or direct financial interest between the author and Y-TEC that could constitute a conflict of interest. The YPF-Tecnología was not involved in the study design, collection, analysis, interpretation of data, the writing of this article or the decision to submit it for publication. The remaining authors declare that the research was conducted in the absence of any commercial or financial relationships that could be construed as a potential conflict of interest.

References

1. Errea, M.I.; Rossi, E.; Goyanes, S.N.; D'Accorso, N.B. Chitosan: From Organic Pollutants to High-Value Polymeric Materials. In *Industrial Applications of Renewable Biomass Products: Past, Present and Future*; Goyanes, S.N., D'Accorso, N.B., Eds.; Springer International Publishing: Cham, Switzerland, 2017; pp. 251–264.

2. Pakizeh, M.; Moradi, A.; Ghassemi, T. Chemical extraction and modification of chitin and chitosan from shrimp shells. *Eur. Polym. J.* **2021**, *159*, 110709. [\[CrossRef\]](#)
3. Yadav, M.; Goswami, P.; Paritosh, K.; Kumar, M.; Pareek, N.; Vivekanand, V. Seafood waste: A source for preparation of commercially employable chitin/chitosan materials. *Bioresour. Bioprocess.* **2019**, *6*, 8. [\[CrossRef\]](#)
4. Díaz Bukvic, G.; Rossi, E.; Errea, M.I. Polysaccharides as Economic and Sustainable Raw Materials for the Preparation of Adsorbents for Water Treatment. *Polysaccharides* **2023**, *4*, 219–255. [\[CrossRef\]](#)
5. Rossi, E.; Ramírez, J.A.Á.; Errea, M.I. Preparation of an environmentally friendly lead adsorbent. A contribution to the rational design of heavy metal adsorbents. *J. Environ. Chem. Eng.* **2020**, *8*, 104210. [\[CrossRef\]](#)
6. Díaz Bukvic, G.; Ojeda Henriquez, M.; Rodríguez Vannini, A.B.; Fidalgo, M.M.; Salvay, A.G.; Rossi, E.; Errea, M.I. Impact of the Three-Dimensional Arrangements of Polyhydroxylated Crosslinkers on the Resulting Properties of Chitosan-Based Hydrogels. *Polysaccharides* **2024**, *5*, 358–379. [\[CrossRef\]](#)
7. Feng, W.; Wang, Z. Tailoring the swelling-shrinkable behavior of hydrogels for biomedical applications. *Adv. Sci.* **2023**, *10*, 2303326.
8. McCarley, R.L. Redox-Responsive Delivery Systems. *Annu. Rev. Anal. Chem.* **2012**, *5*, 391–411. [\[CrossRef\]](#)
9. Swaisgood, H.E. The importance of disulfide bridging. *Biotechnol. Adv.* **2005**, *23*, 71–73. [\[CrossRef\]](#)
10. Altinbasak, I.; Arslan, M.; Sanyal, R.; Sanyal, A. Pyridyl disulfide-based thiol–disulfide exchange reaction: Shaping the design of redox-responsive polymeric materials. *Polym. Chem.* **2020**, *11*, 7603–7624. [\[CrossRef\]](#)
11. Zhao, M.; Li, P.; Zhou, H.; Hao, L.; Chen, H.; Zhou, X. pH/redox dual responsive from natural polymer-based nanoparticles for on-demand delivery of pesticides. *Chem. Eng. J.* **2022**, *435*, 134861. [\[CrossRef\]](#)
12. Peteu, S.F.; Oancea, F.; Siciua, O.A.; Constantinescu, F.; Dinu, S. Responsive Polymers for Crop Protection. *Polymers* **2010**, *2*, 229–251. [\[CrossRef\]](#)
13. Campbell, C. Advances in testing and monitoring of biocides in oil and gas. In *Trends Oil Gas Corrosion Research and Technologies*; Woodhead Publishing: Cambridge, UK, 2017; pp. 489–511.
14. Greene, E.A.; Brunelle, V.; Jenneman, G.E.; Voordouw, G. Synergistic inhibition of microbial sulfide production by combinations of the metabolic inhibitor nitrite and biocides. *Appl. Environ. Microbiol.* **2006**, *72*, 7897–7901. [\[CrossRef\]](#) [\[PubMed\]](#)
15. Huo, M.; Yuan, J.; Tao, L.; Wei, Y. Redox-responsive polymers for drug delivery: From molecular design to applications. *Polym. Chem.* **2014**, *5*, 1519–1528. [\[CrossRef\]](#)
16. Zhang, X.; Han, L.; Liu, M.; Wang, K.; Tao, L.; Wan, Q.; Wei, Y. Recent progress and advances in redox-responsive polymers as controlled delivery nanoplateforms. *Mater. Chem. Front.* **2017**, *1*, 807–822. [\[CrossRef\]](#)
17. Rasheed, P.A.; Jabbar, K.A.; Mackey, H.R.; Mahmoud, K.A. Recent advancements of nanomaterials as coatings and biocides for the inhibition of sulfate reducing bacteria induced corrosion. *Curr. Opin. Chem. Eng.* **2019**, *25*, 35–42. [\[CrossRef\]](#)
18. Lombardo, G.; Dorm, B.C.; Salvay, A.G.; Franzi, L.; Gaffney, M.L.; Peredo Camio, J.B.; Trovatti, E.; Rossi, E.; Errea, M.I. Novel chitosan-based hydrogels as promising wound dressing materials with advanced properties. *Int. J. Biol. Macromol.* **2024**, *279*, 135423. [\[CrossRef\]](#)
19. Kasaai, M.R. Various Methods for Determination of the Degree of N-Acetylation of Chitin and Chitosan: A Review. *J. Agric. Food Chem.* **2009**, *57*, 1667–1676. [\[CrossRef\]](#) [\[PubMed\]](#)
20. Younes, I.; Rinaudo, M. Chitin and Chitosan Preparation from Marine Sources. Structure, Properties and Applications. *Mar. Drugs* **2015**, *13*, 1133–1174. [\[CrossRef\]](#)
21. Pathak, V.; Ambrose, R.P.K. Starch-based biodegradable hydrogel as seed coating for corn to improve early growth under water shortage. *J. Appl. Polym. Sci.* **2020**, *137*, 48523. [\[CrossRef\]](#)
22. Krauland, A.H.; Guggi, D.; Bernkop-Schnürch, A. Oral insulin delivery: The potential of thiolated chitosan-insulin tablets on non-diabetic rats. *J. Control. Release* **2004**, *95*, 547–555. [\[CrossRef\]](#)
23. Hou, X.; Li, Y.; Pan, Y.; Jin, Y.; Xiao, H. Controlled release of agrochemicals and heavy metal ion capture dual-functional redox-responsive hydrogel for soil remediation. *Chem. Commun.* **2018**, *54*, 13714–13717. [\[CrossRef\]](#)
24. Liu, Y.; Yang, G.; Jin, S.; Xu, L.; Zhao, C.-X. Development of High-Drug-Loading Nanoparticles. *ChemPlusChem* **2020**, *85*, 2143–2157. [\[CrossRef\]](#)
25. Labranche, L.-P.; Dumont, S.N.; Levesque, S.; Carrier, A. Rapid determination of total benzalkonium chloride content in ophthalmic formulation. *J. Pharm. Biomed. Anal.* **2007**, *43*, 989–993. [\[CrossRef\]](#)
26. Jones, A.A.; Piloni, G.; Claypool, J.T.; Paiva, A.R.; Summers, Z.M. Evidence of sporulation capability of the ubiquitous oil reservoir microbe *Halanaerobium congolense*. *Geomicrobiol. J.* **2021**, *38*, 283–293. [\[CrossRef\]](#)
27. Pagliaricci, M.; Rojas, G.; Massello, F.L.; Dos Santos, J.; Bortoli, E.; Navarrete, S.; Morris, W.; Vargas, W.; Vega, I. Microbiologically Influenced Corrosion in Unconventional Oil and Gas Facilities: A Tailored Integral Solution. *SPE J.* **2025**, *30*, 5712–5724. [\[CrossRef\]](#)
28. ASTM D7687-17; Standard Test Method for Measurement of Cellular Adenosine Triphosphate in Fuel and Fuel-Associated Water With Sample Concentration by Filtration. ASTM International: West Conshohocken, PA, USA, 2017. [\[CrossRef\]](#)

29. Kumirska, J.; Czerwicka, M.; Kaczyński, Z.; Bychowska, A.; Brzozowski, K.; Thöming, J.; Stepnowski, P. Application of Spectroscopic Methods for Structural Analysis of Chitin and Chitosan. *Mar. Drugs* **2010**, *8*, 1567–1636. [[CrossRef](#)] [[PubMed](#)]
30. Nagano, N.; Ota, M.; Nishikawa, K. Strong hydrophobic nature of cysteine residues in proteins. *FEBS Lett.* **1999**, *458*, 69–71. [[CrossRef](#)] [[PubMed](#)]
31. Ou, K.; Dong, X.; Qin, C.; Ji, X.; He, J. Properties and toughening mechanisms of PVA/PAM double-network hydrogels prepared by freeze-thawing and anneal-swelling. *Mater. Sci. Eng. C* **2017**, *77*, 1017–1026. [[CrossRef](#)]
32. Massarelli, E.; Silva, D.; Pimenta, A.F.R.; Fernandes, A.I.; Mata, J.L.G.; Armês, H.; Salema-Oom, M.; Saramago, B.; Serro, A.P. Polyvinyl alcohol/chitosan wound dressings loaded with antiseptics. *Int. J. Pharm.* **2021**, *593*, 120110. [[CrossRef](#)]
33. Lu, J.; Chen, Y.; Ding, M.; Fan, X.; Hu, J.; Chen, Y.; Li, J.; Li, Z.; Liu, W. A 4arm-PEG macromolecule crosslinked chitosan hydrogels as antibacterial wound dressing. *Carbohydr. Polym.* **2022**, *277*, 118871. [[CrossRef](#)]
34. Hu, M.; Yang, J.; Xu, J. Structural and biological investigation of chitosan/hyaluronic acid with silanized-hydroxypropyl methylcellulose as an injectable reinforced interpenetrating network hydrogel for cartilage tissue engineering. *Drug Deliv.* **2021**, *28*, 607–619. [[CrossRef](#)] [[PubMed](#)]
35. Stojkov, G.; Niyazov, Z.; Picchioni, F.; Bose, R.K. Relationship between Structure and Rheology of Hydrogels for Various Applications. *Gels* **2021**, *7*, 255. [[CrossRef](#)]
36. Mahanta, N.; Teow, Y.; Valiyaveetil, S. Viscoelastic hydrogels from poly(vinyl alcohol)–Fe(iii) complex. *Biomater. Sci.* **2013**, *1*, 519–527. [[CrossRef](#)] [[PubMed](#)]
37. Balouiri, M.; Sadiki, M.; Ibsouda, S.K. Methods for in vitro evaluating antimicrobial activity: A review. *J. Pharm. Anal.* **2016**, *6*, 71–79. [[CrossRef](#)] [[PubMed](#)]

Disclaimer/Publisher’s Note: The statements, opinions and data contained in all publications are solely those of the individual author(s) and contributor(s) and not of MDPI and/or the editor(s). MDPI and/or the editor(s) disclaim responsibility for any injury to people or property resulting from any ideas, methods, instructions or products referred to in the content.